



UNIVERSIDADE ESTADUAL DE CAMPINAS  
SISTEMA DE BIBLIOTECAS DA UNICAMP  
REPOSITÓRIO DA PRODUÇÃO CIENTÍFICA E INTELLECTUAL DA UNICAMP

**Versão do arquivo anexado / Version of attached file:**

Versão do Editor / Published Version

**Mais informações no site da editora / Further information on publisher's website:**

<https://pubs.rsc.org/en/Content/ArticleLanding/2015/RA/c5ra10960d>

**DOI: 10.1039/C5RA10960D**

**Direitos autorais / Publisher's copyright statement:**

©2015 by RSC advances. All rights reserved.

DIRETORIA DE TRATAMENTO DA INFORMAÇÃO

Cidade Universitária Zeferino Vaz Barão Geraldo

CEP 13083-970 – Campinas SP

Fone: (19) 3521-6493

<http://www.repositorio.unicamp.br>



CrossMark  
click for updates

Cite this: *RSC Adv.*, 2015, 5, 62220

# Experimental, DFT and docking simulations of the binding of diapocynin to human serum albumin: induced circular dichroism†

Diego Venturini,<sup>a</sup> Bruna Pastrello,<sup>a</sup> Maria Luiza Zeraik,<sup>b</sup> Ivani Pauli,<sup>c</sup> Adriano Defini Andricopulo,<sup>c</sup> Luiz Carlos Silva-Filho,<sup>a</sup> V. S. Bolzani,<sup>b</sup> Nelson Henrique Morgon,<sup>d</sup> A. R. da Souza<sup>a</sup> and Valdecir Farias Ximenes<sup>\*a</sup>

Diapocynin has been regarded as the active principle of apocynin, which is the most used inhibitor of NADPH oxidase. Here we performed a comprehensive study of the interaction of diapocynin with human serum albumin (HSA). We found that diapocynin binds with higher efficacy to site I of HSA and its binding constant ( $8.5 \times 10^5 \text{ mol}^{-1} \text{ L}$ ) was almost 100-fold higher compared to apocynin. By interacting with this chiral cavity of the protein, diapocynin became a chiral molecule, which was evidenced by its induced circular dichroism spectrum. The axial chirality was theoretically confirmed by searching the most stable conformations adopted by diapocynin using Density Functional Theory (DFT). The four minimum energy conformers, which presented dihedral angles of  $58.00^\circ$  and  $302.00^\circ$  (*syn-aS* and *syn-aR* enantiomers pair bearing 2,2'-dihydroxyl groups at the same side) and  $132.86^\circ$  and  $227.14^\circ$  (*anti-aS* and *anti-aR* enantiomers pair bearing 2,2'-dihydroxyl groups at opposite sides) were used as initial conformations for the docking simulations. The highest scored docking pose was obtained for site 1 and the dihedral angle was  $106.44^\circ$ , *i.e.*, an *anti-aS* chiral conformer. In conclusion, diapocynin is a strong ligand of HSA. An unprecedented combination of DFT calculation and docking simulation was used to explain the acquired chirality of diapocynin when bound to HSA.

Received 9th June 2015  
Accepted 13th July 2015

DOI: 10.1039/c5ra10960d

[www.rsc.org/advances](http://www.rsc.org/advances)

## 1. Introduction

Diapocynin is the dimeric product generated by the oxidation of apocynin.<sup>1</sup> Apocynin has been widely used as an NADPH oxidase (NOX) inhibitor and its beneficial health properties have been demonstrated in an increasing number of publications, including many *in vivo* studies.<sup>2</sup> Some very recent findings include the improvement of the renal glutathione status in Zucker diabetic fatty rats,<sup>3</sup> inhibition of haemodynamic changes in cisplatin-induced cardiotoxicity in rats<sup>4</sup> and a protective effect in a mouse model of chemically-induced colitis.<sup>5</sup> Structurally, apocynin is a very simple molecule. Actually, we believe that without the ancient pharmacological

applications of the herb *Picrorhiza kurroa* in the folk medicine and the posterior isolation of apocynin as one of its active principles,<sup>6–8</sup> this molecule would never have been tested as a potential drug. Indeed, apocynin could be considered a simple precursor for the synthesis of more complex molecules.

Diapocynin is not found in natural products, and only gained importance when Johnson and co-workers demonstrated that the inhibitory capacity of apocynin was linked to its previous peroxidase-mediated oxidation, leading to diapocynin.<sup>1</sup> Subsequently, we demonstrated that diapocynin could be produced when neutrophils were incubated with apocynin and stimulated by phorbol myristate acetate.<sup>9</sup> Currently, not only apocynin, but also diapocynin have been synthesised and used in many experimental models, including a very recent demonstration of its application in the prevention of early Parkinson's disease symptoms in a transgenic mouse model.<sup>10</sup>

Human serum albumin (HSA) is the predominant protein in blood plasma, and one of its main functions is carrying a large diversity of hydrophobic endogenous and exogenous molecules, including many pharmaceutical drugs. To perform that, HSA has binding sites, which are cavities in the protein where the drugs are bound. Hence, binding constants are usually determined for newly-developed drugs as a parameter for the

<sup>a</sup>Department of Chemistry, Faculty of Sciences, São Paulo State University (UNESP), P. O. Box 473, 17033-360, Bauru, São Paulo, Brazil. E-mail: vfximenes@fc.unesp.br; Tel: +55 14 3301 6088

<sup>b</sup>Nuclei of Bioassays, Ecophysiology and Biosynthesis of Natural Products (NuBBE), Department of Organic Chemistry, Institute of Chemistry, São Paulo State University (UNESP), 14800-900, Araraquara, São Paulo, Brazil

<sup>c</sup>Computational and Medicinal Chemistry Laboratory, Physics Institute of São Carlos, University of São Paulo (USP), 13563-120, São Carlos, São Paulo, Brazil

<sup>d</sup>Department of Chemistry, Institute of Chemistry, Campinas State University (UNICAMP), 13083-861, Campinas, São Paulo, Brazil

† Electronic supplementary information (ESI) available. See DOI: 10.1039/c5ra10960d

elucidation of their pharmacodynamic and pharmacokinetic properties.<sup>11</sup>

Diapocynin has a 2,2'-disubstituted-biphenyl moiety; hence, any energy barrier that impedes free rotation around the central single bond between the phenyl rings could provoke the appearance of chirality in this molecule, specifically, axial chirality.<sup>12</sup> This phenomenon is known as induced chirality and is experimentally detected by the appearance of a new circular dichroism signal, which is not present in the protein itself or in the free compound in aqueous solution. This CD signal is named induced circular dichroism spectrum (ICD) and results from the attachment of the optically inactive compound inside the asymmetric microenvironment, which forms the protein binding sites.<sup>13</sup> The appearance of ICD is a quite specific property, since it depends on effective binding between the ligand and the protein and also of a specific alteration in its molecular structure, leading to the conversion of its achiral to chiral conformation, in other words, from an optically inactive to active compound.

As described above, the biomedical application of diapocynin has increased; hence, its potential interaction with HSA must be elucidated, since it could represent a pathway for its distribution in the human body. For these reasons, in this report, our goal was to study the interaction of diapocynin with HSA. The focus was the determination of the binding constant, the search for evidence of induced circular dichroism in diapocynin, the theoretical studies and determination of protein-ligand conformations through docking simulations that could explain the induced chirality.

## 2. Experimental section

### 2.1. Chemicals

Human serum albumin free of fatty acids (HSA), apocynin (4'-hydroxy-3'-methoxyacetophenone), potassium persulphate, ammonium iron(II) sulphate hexahydrate, ibuprofen and warfarin were purchased from Sigma-Aldrich Chemical Co. (St. Louis, MO, USA). Stock solutions of diapocynin and apocynin (10 mM) were prepared in dimethyl sulphoxide. From that, working solutions were prepared by dilution in 50 mM phosphate buffer at pH 7.0. HSA was dissolved in 50 mM phosphate buffer at pH 7.0 to give a 1 mM stock solution, which was stored at 4 °C. Protein concentration was determined by measuring its absorbance at 280 nm ( $\epsilon_{280\text{nm}} = 35\,219\text{ M}^{-1}\text{ cm}^{-1}$ )<sup>14</sup> on a Perkin Elmer Lambda 35 UV-visible spectrophotometer (Shelton, CT, USA). Stock solution of ibuprofen and warfarin (10 mM) were prepared in ethyl alcohol.

### 2.2. Synthesis and characterisation of diapocynin

Diapocynin (1,1'-(6,6'-dihydroxy-5,5'-dimethoxy[1,1'-biphenyl]-3,3'-diyl)bis-ethanone) was prepared as previously described, with slight modifications.<sup>15</sup> Apocynin (1.0 g, 6 mmol) was dissolved in 200 mL of hot water. Next, the heating was turned off and ammonium iron(II) sulphate hexahydrate (118 mg, 0.3 mmol) and potassium persulphate (811 mg, 3.0 mmol) were added and stirred for 30 min. The precipitated product was filtered and washed with

cold water. Then, the product was re-dissolved by adding sodium hydroxide (50 mL, 4 mol L<sup>-1</sup>) and filtered. The brown solution was acidified by adding hydrochloric acid (50 mL, 4 mol L<sup>-1</sup>). The precipitate was filtered and washed with cold water. The product was dried in a vacuum over phosphorus pentoxide, yielding 0.65 g (66%) of a yellow solid. The purity was confirmed by HPLC analysis and was higher than 98%. The analysis was performed by HPLC in line with a diode array detector set at 254 nm (Jasco, Tokyo, Japan). The analyses were carried on a Luna C18 reversed-phase column (250 × 4.6 mm, 5 μm) using solvent A (aqueous formic acid 0.1%) as a mobile phase and solvent B (formic acid 0.1% in acetonitrile). The gradient was: solvent A 90 to 10% in 22 min. The flow rate was 1 mL min<sup>-1</sup>. NMR spectra (CDCl<sub>3</sub> and DMSO-D<sub>6</sub> solutions) were obtained using tetramethylsilane as an internal reference for <sup>1</sup>H and DMSO-D<sub>6</sub> as an internal reference for <sup>13</sup>C (Bruker DRX 400 spectrometer, MA, USA). <sup>1</sup>H NMR (400 MHz, CDCl<sub>3</sub>) δ (ppm): 7.58–7.64 (m, 4H), 6.32 (s, 2OH), 4.02 (s, 6H), 2.58 (s, 6H). <sup>1</sup>H NMR (400 MHz, DMSO-D<sub>6</sub>) δ (ppm): 9.48 (s, 2OH), 7.48 (d, 2H, *J* = 2.0 Hz), 7.46 (d, 2H, *J* = 2.0 Hz), 3.91 (s, 6H), 2.51 (s, 6H). <sup>13</sup>C NMR (100 MHz, DMSO-D<sub>6</sub>) δ (ppm): 196.2 (2C=O), 149.1 (2C), 147.4 (2C), 127.9 (2C), 125.3 (2CH), 124.4 (2C), 109.6 (2CH), 56.0 (2CH<sub>3</sub>), 26.3 (2CH<sub>3</sub>). Mass spectra were obtained using a triple quadrupole mass spectrometer equipped with an electrospray ionisation (ESI) probe (AB Sciex 4500, MA, USA) MS *m/z*: 331 (M + H)<sup>+</sup>, 289, 247, 215, 183, 144 (ESI<sup>+</sup>).

### 2.3. Determination of binding constants

The absorbance and fluorescence spectra were measured using a Perkin Elmer Lambda 35 UV-visible spectrophotometer and Perkin Elmer LS 55 spectrofluorimeter, respectively (Shelton, CT, USA). The fluorescence experiments were performed with the following settings: excitation at 280 nm and emission scanning between 310 and 450 nm. The slit widths were 2.5 nm for excitation and 10 nm for emission wavelengths. A 3 mL quartz cuvette with a 10 mm path length and a magnetic stirrer were used during the measurements. Fluorescence quenching experiments were performed by titration of HSA (5 μM) with diapocynin (0–16 μM) in 50 mM phosphate buffer, pH 7.0, at different temperatures. After each addition, the protein/ligand mixtures were incubated for 2 min before the fluorescence measurements. The fluorescent intensity was corrected for the inner filter effect caused by attenuation of the excitation and emission signals resulting from the absorption of diapocynin, using the following equation:<sup>16</sup>

$$F_{\text{corr}} = F_{\text{obs}} 10^{(A_{\text{bex}} + A_{\text{bem}})/2} \quad (1)$$

where:  $F_{\text{corr}}$  and  $F_{\text{obs}}$  are the corrected and observed fluorescence intensities, respectively; and  $A_{\text{bex}}$  and  $A_{\text{bem}}$  are the absorptions of the mixture at excitation (280 nm) and emission wavelengths (343 nm), respectively.

### 2.4. Far and near-UV circular dichroism experiments

Circular Dichroism (CD) spectra were recorded with a Jasco J-815 spectropolarimeter (Jasco, Japan) equipped with a thermostatically controlled cell holder. The spectra were obtained

with 1 nm step resolution, response time of 1 s and scanning speed of 50 nm min<sup>-1</sup>. For the far-UV CD experiments, HSA (30 μM) and, when present, apocynin or diapocynin (30 μM) were incubated for 30 min at 25 °C and then diluted to 2 μM and the spectra recorded in the range 195–250 nm using a 2 mm path length quartz cuvette.

The near-UV CD spectra were recorded at HSA 30 μM and apocynin or diapocynin 30 μM over a wavelength range of 250–450 nm at 25 °C. A 3 mL quartz cuvette with a 10 mm path length and a magnetic stirrer were used for the measurements in the near-UV-CD range. The baseline (50 mM phosphate buffer) was subtracted from all measurements.

## 2.5. Theoretical studies

In this study, we employed the quantum chemical formalism at the *ab initio* level using the Density Functional Theory (DFT) approach to understanding the experimental results. The search for the most stable conformation adopted by diapocynin, in the gas phase, was carried out at the M06-2X/6-31G(d) level of theory. All computer simulations were done in the GridUnesp supercomputer facilities, which is composed of 256 SUN X4150 servers with 2048 cores (Intel Xeon 2.83 GHz), with 4096 GB of RAM memory (2 GB per core) and an infiniband 4X DDR (20 Gbps) connection. The storage capacity of these system is 36 TB through DAS optical fibre (StorageTek 6140) and 96 TB at four SUN X4500 servers. The Gaussian 09 (ref. 17) suite of programs was employed to obtain the geometric and energy parameters for diapocynin.

## 2.6. Docking simulations

Simulations were carried out using GOLD 5.2 (Genetic Optimization for Ligand Docking), a software based on a genetic algorithm to explore the ligand conformational space. HSA protein coordinates were obtained from 2BXF (2.9 Å resolution) available at the Protein Data Bank (PDB).<sup>18,19</sup> HSA was prepared for docking studies by adding hydrogen atoms, removing water and co-crystallized inhibitors. Initial conformations of diapocynin molecules, differing on their dihedral angles (58.00°, 132.86°, 227.14° and 302.00°), were docked in both binding sites of HSA (site 1 and site 2). In all simulations the protein was kept fixed, while the ligand was treated as fully flexible. Protein–ligand interactions within a radius of 12 Å were evaluated. The sphere was centered on TYR150 phenol oxygen atom in site 1, and on TYR411 phenol oxygen in site 2. Docking poses were ranked by the ChemPLP scoring function, available in the GOLD 5.2 package, which was also used to choose the representative conformation for each ligand. Score scale gives a guide of how good the pose is (the higher the score, the better the docking result is likely to be). ChemPLP is the most recently scoring function introduced in GOLD.<sup>20</sup> This simple potential has both an attractive and repulsive part for neutral contacts and solely a repulsive part for anti-complementary contacts (donor–donor, metal–donor and acceptor–acceptor). Chemscore hydrogen bonding term is used for hydrogen bonds and internal energy.<sup>21,22</sup> Besides, all solutions found by the program were visually inspected for mutual (protein and ligand) surface

complementarity and the presence of unfilled space at the complex interface. Ligplot was used to identify contacts among ligands and HSA.<sup>23</sup>

## 3. Results and discussion

### 3.1. Synthesis and characterisation of diapocynin

Diapocynin can be produced by enzymatic and non-enzymatic catalysed oxidations of apocynin (Fig. 1).<sup>15,24</sup> In this regard, the neutrophil peroxidase, myeloperoxidase, is supposed to be the enzyme involved in its endogenous production.<sup>9</sup> Here, diapocynin was synthesised by ferrous sulphate-catalysed oxidation of apocynin using sodium persulphate as the oxidising agent. Its purity (>98%) was evaluated by HPLC and its identity by NMR and mass spectroscopy (ESI<sup>+</sup>). Since our studies involved the determination of binding constants using spectroscopy techniques, we also determined the absorption spectra and the molar absorptivity coefficients of diapocynin in 50 mM phosphate buffer pH 7.0 at 270 nm ( $2.35 \pm 0.02 \times 10^4 \text{ M}^{-1} \text{ cm}^{-1}$ ) and 303 nm ( $1.91 \pm 0.01 \times 10^4 \text{ M}^{-1} \text{ cm}^{-1}$ ) (ESI<sup>+</sup>). These analytical data can be useful for researchers interested in the quantification of diapocynin.

### 3.2. Determination of the binding constant

The analytical approach that we used for measuring the interaction between HSA and diapocynin was fluorescence quenching, a phenomenon associated with the decrease in the fluorescence intensity caused by collisional deactivation (dynamic quenching), and formation of a ground-state complex (static quenching), among other mechanisms.<sup>16</sup> The results in Fig. 2(a) show that the fluorescence intensity of HSA was strongly decreased by the addition of diapocynin, reaching almost complete suppression at only 3 molar excess of the quencher. The linear relationship obtained using the Stern–Volmer equation (eqn (2), Fig. 2(b)) is an indication that only one mechanism of quenching is involved in suppression of the fluorescence in the experimental condition used here.<sup>25</sup>

$$F_0/F = 1 + K_{sv}[Q] \quad (2)$$

In this equation,  $F_0$  and  $F$  are the fluorescence intensity of HSA in the absence and presence of the diapocynin, respectively,  $K_{sv}$  is the Stern–Volmer constant and  $[Q]$  is the concentration of diapocynin (quencher). The evidence that the

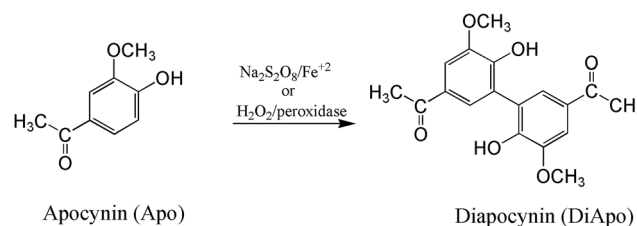


Fig. 1 Chemical equation for the enzymatic or non-enzymatic preparation of diapocynin from apocynin.

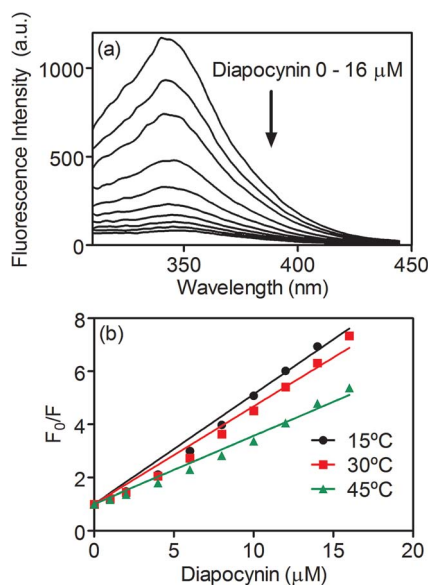


Fig. 2 Emission spectra of HSA in the absence or presence of diapocynin. (a) Emission spectra of 5  $\mu\text{M}$  HSA in the absence or presence of diapocynin (0–16  $\mu\text{M}$ ) in 0.05 M phosphate buffer at pH 7.0. (b) Stern–Volmer plots at different temperatures ( $\lambda_{\text{ex}} = 280 \text{ nm}$ ,  $\lambda_{\text{em}} = 343 \text{ nm}$ ). The results are the average and SD of experiments performed in triplicate.

Table 1 Stern–Volmer and binding constants for the interaction between diapocynin and human serum albumin<sup>a</sup>

$T$ ( $^{\circ}\text{C}$ )	$K_{\text{sv}}$ ( $10^5 \text{ mol}^{-1} \text{ L}$ )	$R^2$	$K_{\text{a}}$ ( $10^6 \text{ mol}^{-1} \text{ L}$ )	$R^2$
15	4.13	0.9919	1.02	0.9982
30	3.70	0.9902	0.85	0.9980
45	2.57	0.9905	0.50	0.9985

<sup>a</sup>  $K_{\text{sv}}$ : Stern–Volmer constant;  $K_{\text{a}}$ : binding constant;  $R^2$ : linear correlation coefficient.

fluorescence quenching resulted from the formation of ground-state complex between diapocynin and HSA was obtained by measuring the effect of temperature on the Stern–Volmer constant. From the results in Fig. 2(b) and Table 1, it can be concluded that the interaction was weakened at higher temperatures, which is a typical characteristic of static quenching provoked by the formation of the ground-state complex.<sup>25</sup>

From these findings, which indicated that HSA is able to complex with diapocynin, the fluorescence quenching experiments were used for the determination of the binding constant ( $K_{\text{a}}$ ) using a non-linear equation (Fig. 3, eqn (3)). This mathematical treatment was chosen because it has been described as the more adequate for experiments where the concentration of the free ligand cannot be assumed as equal to the added ligand, which is the case here, since only three molar excess of diapocynin was able to quench practically all the fluorescence of HSA:<sup>16,26</sup>

$$F/F_0 = 1 - \Phi[(K_{\text{d}} + nP_0 + L) - \text{sqr}((K_{\text{d}} + nP_0 + L)^2 - (4nP_0L))]/2nP_0 \quad (3)$$

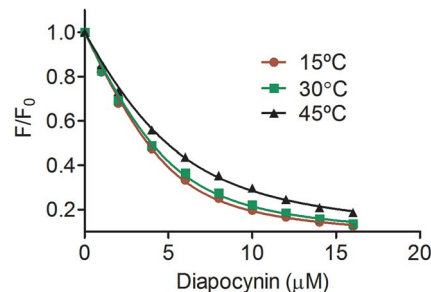


Fig. 3 Complexation between HSA and diapocynin. Non-linear fitting for determination of the binding constant ( $K_{\text{a}}$ ) at different temperatures. The results are the average and SD of experiments performed in triplicate.

where:

$F_0$ : fluorescence in the absence of ligand;

$F$ : fluorescence in the presence of ligand;

$\Phi$ : fluorescence ratio amplitude ( $1 - F_{\text{ratio}\infty}$ );

$F_{\text{ratio}}$ : ( $F/F_0$ );

$F_{\text{ratio}\infty}$ :  $F_{\text{ratio}}$  at infinite concentration of the ligand;

$P_0$ : protein concentration;

$L$ : added ligand;

$K_{\text{d}}$ : dissociation constant;

$K_{\text{a}} = 1/K_{\text{d}}$ ;

$n$ : stoichiometry of the binding.

The stoichiometry of the binding was assumed as one, which was the value obtained by fitting the data in the double logarithm regression equation (ESI<sup>†</sup>). Therefore, only  $K_{\text{d}}$  and  $\Phi$  were treated as the fitting parameters in the nonlinear least-squares analysis (GraphPad Prism version 5.00 for Windows, GraphPad Software, San Diego California USA). The value obtained for  $K_{\text{a}}$  for diapocynin at 30  $^{\circ}\text{C}$  ( $8.5 \times 10^5 \text{ mol}^{-1} \text{ L}$ , Fig. 3, Table 1) is significantly higher compared to the reported value for apocynin ( $2.2 \times 10^4 \text{ mol}^{-1} \text{ L}$ ),<sup>27</sup> which is an indication of its stronger association with HSA.

Considering that diapocynin have been proposed as the pharmacologically-active form of apocynin,<sup>1,9,10,27–29</sup> this finding could have important implications for the comprehension of its mechanism of action and pharmacokinetic properties. For this reason, we performed additional experiments that could provide further details regarding the interaction between HSA and diapocynin.

### 3.3. Interaction of diapocynin with HSA: induced circular dichroism studies

Since diapocynin was a strong ligand of HSA, we also investigated whether this interaction could alter the secondary structure of the protein. Thus, the far-UV CD spectra of the protein were measured in the presence or absence of diapocynin. The results depicted in Fig. 4(a) show the typical CD spectrum of HSA with the minimums at 208 and 222 nm.<sup>30</sup> As can be observed, the presence of diapocynin did not alter the spectral pattern of the secondary structure of HSA.

The near-UV CD spectrum of HSA in the presence or absence of diapocynin was also studied. The results in Fig. 4(b) show the

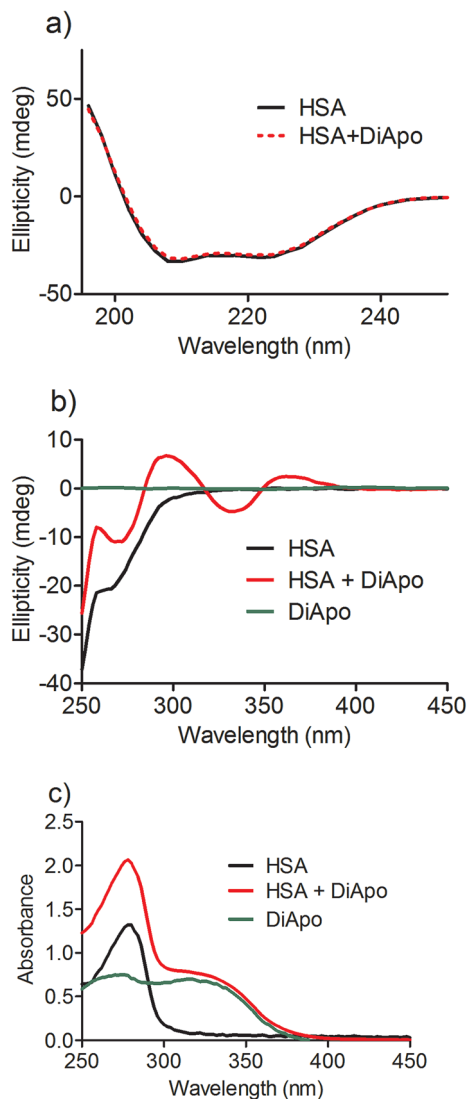


Fig. 4 (a) Far-UV-CD spectrum of HSA and the effect of diapocynin. (b) HSA-induced ellipticity in diapocynin (DiApo). (c) UV-Vis spectra of HSA in the presence or absence of diapocynin. The mixtures consisted of 30  $\mu\text{M}$  HSA and 30  $\mu\text{M}$  ligands in 0.05 M phosphate buffer at pH 7.0. For far-UV-CD experiments the samples were diluted to 2  $\mu\text{M}$  before the measurements.

UV absorption band of diapocynin, but the lack of any CD signal, as could be expected for an achiral molecule. How could also be expected, HSA alone presented its typical band below 300 nm.<sup>31</sup> However, when diapocynin was added to HSA in equimolar amounts, a new CD band was obtained, which was dependent of the presence of both, HSA and diapocynin.

This new CD signal, *i.e.*, an induced CD (ICD), can be attributed as an induced chirality in diapocynin provoked by its binding in HSA. In other words, the achiral diapocynin became chiral when complexed with the protein. How well-known, this phenomenon can be explained as the result of the attachment of an optically inactive molecule inside the chiral microenvironment, which forms the proteins binding sites.<sup>13</sup> Obviously, this finding is an additional and unequivocal confirmation that diapocynin was complexed with HSA.

Interestingly, apocynin, alone or complexed with the protein, did not show any ICD signal (ESI<sup>†</sup>). Considering that from a structural point of view, the major difference between apocynin and diapocynin is the biphenyl moiety, which enables the rotation around the single for the last; the absence of induced chirality in apocynin suggests that axial chirality must be involved in the ICD of diapocynin.

#### 3.4. Determination of diapocynin binding site on HSA: application of the ICD signal

So far, we have demonstrated that diapocynin is a strong ligand of HSA and its complexation provoked the induction of chirality. Thus, we decided to use this ICD signal to probe the location of diapocynin in HSA. It is worthy of note that HSA has two main binding sites, which are known as warfarin binding site (site I) and benzodiazepine binding site (site II).<sup>32</sup> Our hypothesis was that by adding specific ligands for these sites, a competition between diapocynin and the ligands by the binding sites of the protein could take place and provokes the decrease in the diapocynin ICD signal. In other words, a typical site-specific marker displacement assay for determination of binding sites, but using the ICD signal and not fluorescence quenching, as usually performed.<sup>33</sup>

The results depicted in Fig. 5(a) show the effect of the addition of warfarin (site I ligand) in an equimolar mixture of HSA and diapocynin. How can be observed, the ICD spectrum of diapocynin (positive band at 300 nm and negative band at 332 nm) was progressively decreased by the addition of warfarin. On the other hand, ibuprofen (site II ligand) provoked opposite effect, since the ICD (negative band at 332 nm) was progressively increased (Fig. 5(b)).

From these results our interpretation was that diapocynin has higher affinity for site I in HSA, but the binding in site II is also possible. This hypothesis was based in the following finding:

(i) The ICD spectrum of diapocynin must be the result of its binding in site I and II;

(ii) The positive band with maximum at 288 nm and the negative band at 332 nm are mainly due to the interaction of diapocynin with site I. How can be observed, these bands were significantly affected by the addition of warfarin, but not by ibuprofen;

(iii) The positive band centered at 366 nm must be mainly due to the diapocynin interaction with site II. How can be observed the addition of ibuprofen provoked a decrease in this band but an increase in the band at 332 nm.

From these findings we propose that the simultaneous increase in the band at 332 and 300 nm and the decrease at 366 nm by the addition of ibuprofen could be the consequence of the displacement of diapocynin from site II to site I. Corroborant with that, the addition of warfarin provoked the decrease in the band at 300 and 332 nm, but not affected the band at 366 nm.

The confirmation that diapocynin had higher affinity for site I, was also obtained by measuring the its binding constant in the absence or presence of warfarin and ibuprofen using the double logarithm equation in the fluorescence quenching experiments (ESI<sup>†</sup>). The binding constants obtained in these

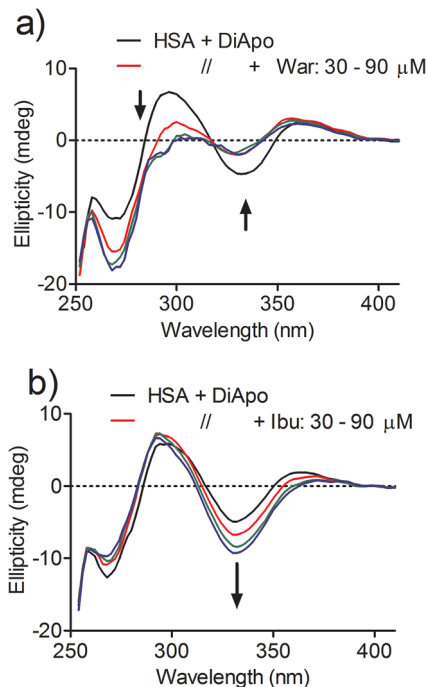


Fig. 5 Displacement of diapocynin from HSA by warfarin (site I) and ibuprofen (site II). The mixtures consisted of 30  $\mu\text{M}$  HSA and 30  $\mu\text{M}$  diapocynin (DiApo) in 0.05 M phosphate buffer at pH 7.0. (a) Addition of warfarin (30 to 90  $\mu\text{M}$ ). (b) Addition of ibuprofen (30 to 90  $\mu\text{M}$ ).

experiments were: diapocynin ( $1.42 \times 10^5 \text{ mol}^{-1} \text{ L}$ ); warfarin + diapocynin ( $6.27 \times 10^5 \text{ mol}^{-1} \text{ L}$ ); ibuprofen + diapocynin ( $1.49 \times 10^5 \text{ mol}^{-1} \text{ L}$ ). The higher alteration of the binding constant in the presence of warfarin is an additional confirmation that diapocynin and warfarin occupies the same binding site.<sup>34</sup>

Finally, it is worthy of note that HSA is not able to induce chirality in warfarin or ibuprofen in this region of the UV-Vis spectrum. Thus, the alterations in the ICD of diapocynin provoked by the addition of these drugs were not the result of superposition of ICD spectra (ESI<sup>†</sup>).

### 3.5. Diapocynin: determination of the minimum energy conformations

The generation of an ICD signal for diapocynin suggested that the stabilised conformation of diapocynin inside the protein HSA should have a non-zero dihedral angle around the single bond that links the two phenyl rings. Thus, to gain further insight in to the reasons that could explain the presence of induced chirality in diapocynin, theoretical studies were performed searching for the most stable conformations of diapocynin. The quantum chemical formalism used to search for the most stable conformations adopted by diapocynin in the gas phase was carried out at the Density Function Theory (DFT) using the M06-2X method along with the 6-31G(d) basis set. The energy for each conformation of diapocynin was obtained and plotted as a function of the dihedral angle using the SCAN keyword available at the Gaussian suite of programs. In these calculations, we obtain a potential energy surface (PES) which consists of single point energy evaluations over a rectangular grid involving the Cartesian

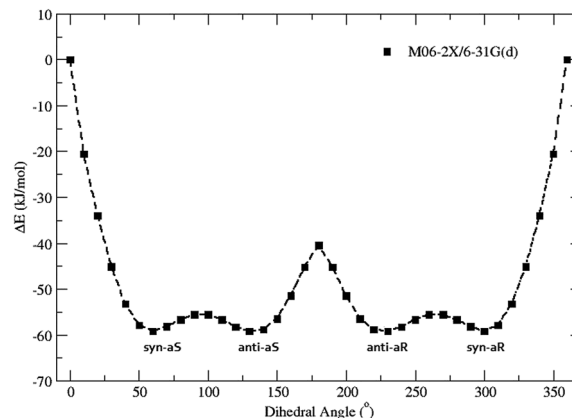


Fig. 6 Energy scan for conformers of diapocynin obtained by M06-2X method along with the 6-31G(d) basis set.

coordinates of diapocynin atoms. The interval and step size was 0 to 360 and 10 degrees, respectively. The minimum energy for diapocynin in the gas phase was obtained by using this methodology. From these minimum energy conformations, optimisation of the diapocynin geometry was performed using a more sophisticated basis set to include polarisation and correlation functions: 6-311++G(d,p). In this methodology of calculations the solvent, water, was included through the Polarised Continuum Medium (PCM) model,<sup>35</sup> and the harmonic vibrational frequency for characterisation of the stationary points was obtained.

Fig. 6 shows the four minimum energy conformations, which presented the dihedral angles at 62.5°, 127.0°, 232.1°, and 300.7° and the three transition states. The reference was the planar structure, which possess a dihedral angle equal to zero and the highest energy. The Cartesian coordinates and thermodynamics parameters for the conformations are available (ESI<sup>†</sup>).

After the optimisation described above, the minimum energy conformations presented the dihedral angles of 58.00°, 132.86°, 227.14° and 302.00° (Fig. 7). It is important to note that the conformers at 58.00° (*syn-aS*) and 302.00° (*syn-aR*) are a pair of enantiomers and presented the same energy (approximately  $-60 \text{ kJ mol}^{-1}$ ). Similarly, the conformers at 132.86° (*anti-aS*) and 227.14° (*anti-aR*) are also a pair of enantiomers and presented the same energy level (Fig. 7).

From these results, it was possible to infer that although the non-planar conformation of diapocynin is significantly more stable compared to the planar one, the energetic barrier for the conversion of the enantiomers, through the transition state at 180°, which was approximately  $20 \text{ kJ mol}^{-1}$  (Fig. 6), is low compared to  $93 \text{ kJ mol}^{-1}$ . This rotation barrier energy value has been established as a minimum for the planar conformation of biaryls, which could impede the interconversion of the enantiomers at room temperature.<sup>36</sup> In conclusion, and in agreement with the experimental results, diapocynin should not have axial chirality when free in aqueous solution.

### 3.6. Diapocynin: docking simulations

According to our experimental findings, diapocynin binds with higher efficacy in site I of HSA. Moreover, diapocynin must

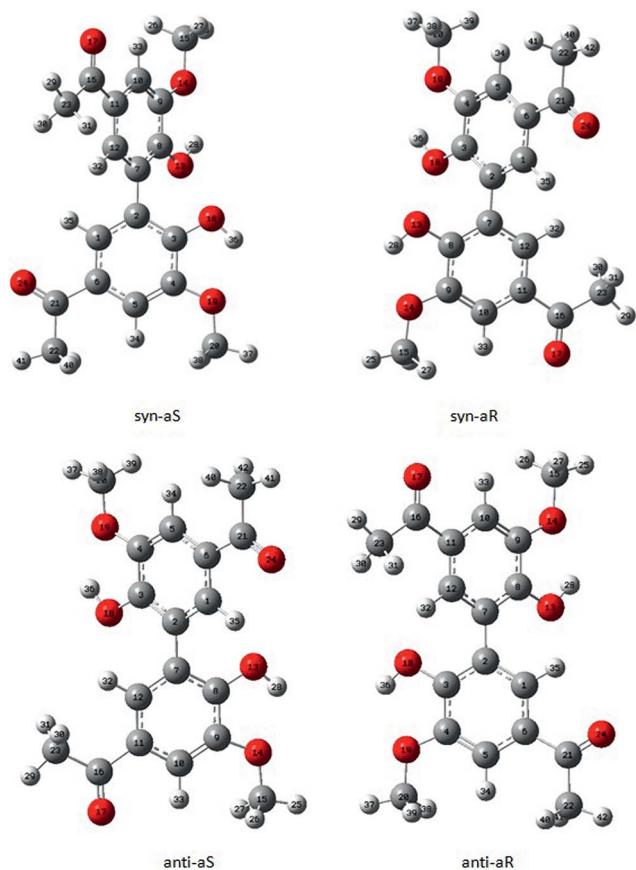


Fig. 7 Minimum energy conformers of diapocynin obtained by M06-2X method along with the 6-311++G(d,p) basis set. Dihedral angle at atoms 3-2-7-8: enantiomers bearing 2,2'-dihydroxyl groups in the same side, *syn-aS* (58.00°) and *syn-aR* (302.00°). Enantiomers bearing 2,2'-dihydroxyl groups in the opposite side, *anti-aS* (132.86°) and *anti-aR* (227.14°).

adopt a non-zero dihedral angle around the single bond that links the phenyl rings, which justify its ICD spectrum. Therefore, docking simulations were performed aiming to obtain the conformations of diapocynin and the scores for its binding in site 1 and site 2. In these experiments, the conformations of diapocynin used for initiation of the docking simulations were that of the minimum energy obtained above, *i.e.*, dihedral angles of 58.00°, 132.86°, 227.14° and 302.0°.

**3.6.1. Docking results for site 1.** Site 1 is a pre-formed binding pocket within the core of subdomain IIA. Inside, the pocket is predominantly apolar, but contains two clusters of polar residues, an inner one towards the bottom of the pocket (TYR150, HIS242, ARG257) and an outer cluster at the pocket entrance (LYS195, LYS199, ARG218, ARG222). The large binding cavity is comprised of a central zone from which three distinct compartments extend. The back end is divided by ILE264 into left and right hydrophobic sub-chambers, whereas a third sub-chamber protrudes from the front of the pocket, delineated by PHE211, TRP214, ALA215, LEU238 and aliphatic portions of LYS199 and ARG218.<sup>19</sup> At site 1, diapocynin binds in the centre of the pocket (Fig. 8), in a very similar way to drugs that are known to bind HSA, such as oxyphenylbutazone,

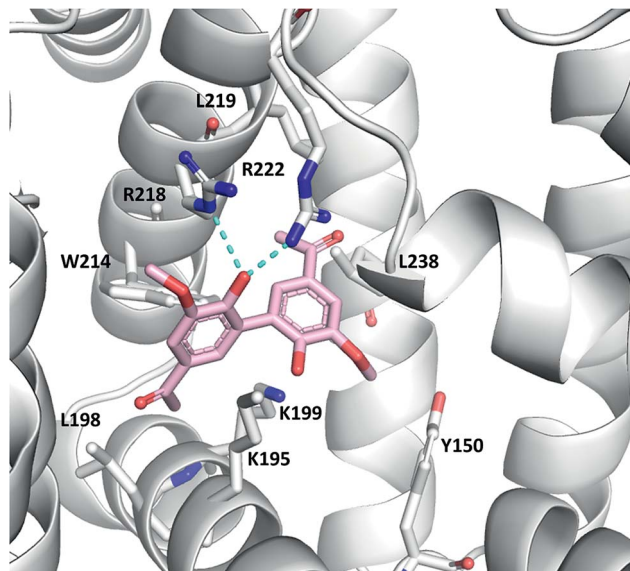


Fig. 8 Docking pose obtained for diapocynin bound to HSA site 1. This frame represents the highest scored conformation at site 1: the dihedral angle around the biphenyl ring is 106.44°. The interactions with the amino acid residues are highlighted. Hydrogen bonds are depicted as cyan dashed lines.

phenylbutazone and warfarin (PDB access codes: 2BXB, 2BXC and 2BXD, respectively). When analysing ChemPLP score values (which account for pose prediction quality) for the top scored solution for each dihedral angle docked to site 1, the lowest value was obtained for angle 132.86° (48.33), followed by angle 302.00° (48.88), then 58.00° (49.68); the highest was obtained for the angle 227.14° (51.13). For this top scored solution, hydrogen bonds (HBs) occurred between diapocynin and the HSA residues ARG218 and ARG222. Hydrophobic contacts involved the protein residues TYR150, GLU153, SER192, LEU238, TRP214, HIS242, ARG257 and ALA291. From this final top scored pose at site 1, the dihedral angle was measured and resulted in 106.44°, *i.e.*, an *anti-aS* chiral conformer.

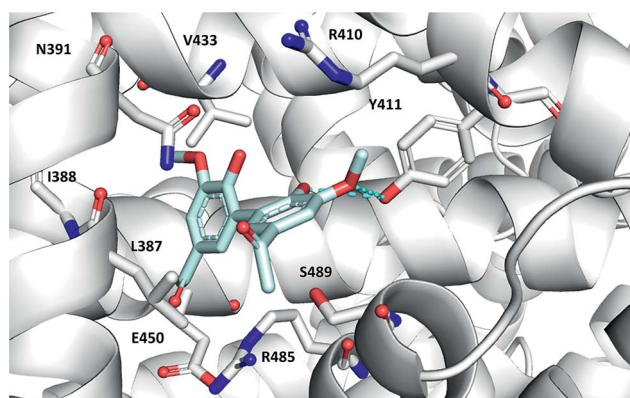


Fig. 9 Docking pose obtained for diapocynin bound to HSA site 2. This frame represents the highest scored conformation at site 2: the dihedral angle around the biphenyl ring is 303.44°. The interactions with the amino acid residues are highlighted. Hydrogen bonds are depicted as cyan dashed lines.

**3.6.2. Docking results for site 2.** Drug site 2 is composed of all six helices of subdomain IIIA and is, therefore, topologically similar to site 1 (subdomain IIA). Although also comprising a largely pre-formed hydrophobic cavity with distinct polar features, there are significant differences between the two drug pockets. Drug site 2 is smaller than site 1; the main binding region corresponds to the central region of site 1 and seems to possess just one sub-compartment, which is only accessed following ligand-induced side-chain movements. In addition, site 2 is more exposed to solvent regarding differences in the way in which HSA subdomains are packed.<sup>19</sup> In contrast to site 1, site 2 has a single main polar patch, located close to one side of the binding pocket entrance and centred on TYR411, but also including ARG410, LYS414 and SER489.

Top scored docking results show that in all diapocynin–HSA complexes one single hydrogen bond takes place between diapocynin and TYR411 phenol oxygen (Fig. 9). Hydrophobic contacts include HSA residues LEU387, ILE388, ASN391, ARG410, TYR411, LYS414, VAL433, GLU450, ARG485, and SER489 depending on the dihedral angle adopted by diapocynin. When analysing ChemPLP score values for the top scored solution for each dihedral angle docked to site 2, the lowest value was obtained for angle 58.00° (41.09), followed by angle 132.86° (41.27), and then 227.14° (43.63); the highest score for docking to site 2 was obtained for the angle 302.00° (44.13). From this final top scored pose at site 2, the dihedral angle was measured and resulted in 303.44°, *i.e.*, a *syn-aR* conformer. By comparing this value with that for site 1 (51.13), it is possible to infer that diapocynin has a preference for binding in site 1 of HSA, which is in accordance with our experimental results.

## 4. Conclusions

Diapocynin is a new, inexpensive, easily prepared and very promising drug with potential applications in the treatment of chronic inflammatory diseases. Here, we demonstrated for the first time that diapocynin is a strong ligand of HSA. Having a binding constant of two orders of magnitude higher compared to the precursor apocynin; the pharmacokinetic properties of diapocynin can be quite different. This finding must be taken into account when these compounds are used *in vivo*.

By interacting with the chiral cavities of the protein diapocynin became a chiral compound, which was evidenced by the induced circular dichroism spectrum, only detected when the protein was added to the reaction medium. In this regard, it is interesting to note that only biaryls bearing voluminous substituents in the proximity of the axial axis can be isolated as pure enantiomers. Obviously, this is not the case for free diapocynin, as we have experimentally and theoretically demonstrated. Thus, it is reasonable to suppose that the interaction with amino acid residues in the binding site may provide a stabilisation of more than 93 kJ mol<sup>-1</sup>, which is a value that has been accepted as the minimum necessary to impede the free rotation of substituted biaryls.<sup>36</sup>

Finally, our experimental and theoretical results showed that diapocynin has higher affinity for site I in HSA and the more

stable conformation presented a dihedral angle of 106.44°, *i.e.*, an *anti-aS* conformer. These experimental and theoretical findings could explain the observed ICD signal.

## Acknowledgements

We gratefully acknowledge financial support from FAPESP (Fundação de Amparo à Pesquisa do Estado de São Paulo, grants #2013/08784-0, #2010/52327-5, #2011/03017-6 and #2013/07600-3), CNPq (Conselho Nacional de Desenvolvimento Científico e Tecnológico), CAPES (Coordenação de Aperfeiçoamento de Pessoal de Nível Superior) and GRIDUNESP.

## References

- 1 D. K. Johnson, K. J. Schillinger, D. M. Kwait, C. V. Hughes, E. J. McNamara, F. Ishmael, R. W. O'Donnell, M. M. Chang, M. G. Hogg, J. S. Dordick, L. Santhanam, L. M. Ziegler and J. A. Holland, *Endothelium*, 2002, **9**, 191–203.
- 2 B. A. Thart, S. Copray and I. Philippens, *BioMed Res. Int.*, 2014, 1–6.
- 3 K. Winiarska, D. Focht, B. Sierakowski, K. Lewankowski, M. Orłowska and M. Usarek, *Chem.–Biol. Interact.*, 2014, **218**, 9–12.
- 4 M. M. El-Sawalhi and L. A. Ahmed, *Chem.–Biol. Interact.*, 2014, **207**, 58–66.
- 5 M. Marín, R. M. Giner, J. L. Ríos and M. D. Recio, *Planta Med.*, 2013, **79**, 1392–1400.
- 6 F. Engels, B. F. Renirie, B. A. Hart, R. P. Labadie and F. P. Nijkamp, *FEBS Lett.*, 1992, **305**, 254–256.
- 7 W. Dorsch and H. Wagner, *Int. Arch. Allergy Appl. Immunol.*, 1991, **94**, 262–264.
- 8 S. Pfuhler, P. Stehrer-Schmid, W. Dorsch, H. Wagner and H. U. Wolf, *Phytomedicine*, 1995, **4**, 319–322.
- 9 V. F. Ximenes, M. K. Kanegae, S. R. Rissato and M. S. Galhiane, *Arch. Biochem. Biophys.*, 2007, **457**, 134–141.
- 10 B. P. Dranka, A. Gifford, A. Ghosh, J. Zielonka, J. Joseph, A. G. Kanthasamy and B. Kalyanaraman, *Neurosci. Lett.*, 2013, **549**, 57–62.
- 11 K. Yamasaki, V. T. Chuang, T. Maruyama and M. Otagiri, *Biochim. Biophys. Acta*, 2013, **1830**, 5435–5443.
- 12 T. Mori, Y. Inoue and S. Grimme, *J. Phys. Chem. A*, 2007, **111**, 4222–4234.
- 13 J. Gawroński and J. Grajewski, *Org. Lett.*, 2003, **18**, 3301–3303.
- 14 C. M. Pace, F. Vajdos, L. Fee, G. Grimsley and T. Gray, *Protein Sci.*, 1995, **11**, 2411–2423.
- 15 M. S. Dasari, K. M. Richards, M. L. Alt, C. F. P. Crawford, A. Schleiden, J. Ingram, A. A. A. Hamiclou, A. Williams, P. A. Chernovitz, R. S. Luo, G. Y. Sun, R. Luchtefeld and R. E. Smith, *J. Chem. Educ.*, 2008, **85**, 411–412.
- 16 S. Roy, *Methods Enzymol.*, 2004, **379**, 175–187.
- 17 M. J. Frisch, G. W. Trucks, H. B. Schlegel, G. E. Scuseria and M. A. Robb, *Gaussian 98*, Gaussian, Pittsburgh, 1998.
- 18 M. L. Verdonk, J. C. Cole, M. J. Hartshorn, C. W. Murray and R. D. Taylor, *Proteins*, 2003, **52**, 609–623.

- 19 J. Ghuman, P. A. Zunszain, I. Petitpas, A. A. Bhattacharya, M. Otagiri and S. Curry, *J. Mol. Biol.*, 2005, **353**, 38–52.
- 20 O. Korb, T. Stütze and T. E. Exner, *J. Chem. Inf. Model.*, 2009, **49**, 84–96.
- 21 M. D. Eldridge, C. W. Murray, T. R. Auton, G. V. Paolini and R. P. Mee, *J. Comput.-Aided Mol. Des.*, 1997, **11**, 425–445.
- 22 M. L. Verdonk, J. C. Cole, M. J. Hartshorn, C. W. Murray and R. D. Taylor, *Proteins*, 2003, **52**, 609–623.
- 23 A. C. Wallace, R. A. Laskowski and J. M. Thornton, *Protein Eng.*, 1995, **8**, 127–134.
- 24 R. T. Nishimura, C. H. Giammanco and D. A. Vosburg, *J. Chem. Educ.*, 2010, **87**, 526–527.
- 25 J. R. Lakowicz, *Principles of Fluorescence Spectroscopy*, Springer, New York, 3rd edn, 2006.
- 26 M. van de Weert and L. Stella, *J. Mol. Struct.*, 2011, **998**, 144–150.
- 27 M. S. Petrônio, M. L. Zeraik, L. M. Fonseca and V. F. Ximenes, *Molecules*, 2013, **18**, 2821–2839.
- 28 H. M. Ismail, L. Scapozza, U. T. Ruegg and O. M. Dorchie, *PLoS One*, 2014, **9**, e110708.
- 29 A. Ghosh, A. Kanthasamy, J. Joseph, V. Anantharam, P. Srivastava, B. P. Dranka, B. Kalyanaraman and A. G. Kanthasamy, *J. Neuroinflammation*, 2012, **9**, 241–256.
- 30 V. I. Dodero, Z. B. Quirolo and M. A. Sequeira, *Front. Biosci., Landmark Ed.*, 2011, **16**, 61–73.
- 31 C. Sun, J. Yang, X. Wu, X. Huang, F. Wang and S. Liu, *Biophys. J.*, 2005, **88**, 3518–3524.
- 32 S. Baroni, M. Mattu, A. Vannini, R. Cipollone, S. Aime, P. Ascenzi and M. Fasano, *Eur. J. Biochem.*, 2001, **268**, 6214–6220.
- 33 H. J. Hu, H. L. Yue, X. L. Li, S. S. Zhang, E. Tang and L. P. Zhang, *J. Photochem. Photobiol., B*, 2012, **112**, 16–22.
- 34 N. Zhoua, L. Yi-Zeng and P. Wanga, *J. Mol. Struct.*, 2008, **872**, 190–196.
- 35 J. Tomasi, B. Mennucci and R. Cammi, *Chem. Rev.*, 2005, **105**, 2999–3094.
- 36 G. Haberhauer, C. Tepper, C. Wölper and D. Bläser, *Eur. J. Org. Chem.*, 2013, **12**, 2325–2333.